Marine Micropaleontology 174 (2022) 101959

Contents lists available at ScienceDirect

Marine Micropaleontology

journal homepage: www.elsevier.com/locate/marmicro

Research paper

Temporal shifts in ostracode sexual dimorphism from the Late Cretaceous to the late Eocene of the U.S. Coastal Plain

Maya Samuels-Fair [a,b], Maria João Fernandes Martins [c], Rowan Lockwood [d], John P. Swaddle [e], Gene Hunt [a,*]

[a] Department of Paleobiology, National Museum of Natural History, Smithsonian Institution, Washington, DC, United States
[b] Department of Integrative Biology, University of California Berkeley, Berkeley, CA, United States
[c] Interdisciplinary Center for Archaeology and Evolution of Human Behaviour, Universidade do Algarve, Faro, Portugal
[d] Department of Geology, College of William & Mary, Williamsburg, VA, United States
[e] Institute for Integrative Conservation, College of William & Mary, Williamsburg, VA, United States

ARTICLE INFO

Keywords:
Ostracoda
Sexual dimorphism
Sexual selection
Paleogene

ABSTRACT

Ostracodes of the superfamily Cytheroidea exhibit sexual dimorphism in the carapace such that males are more elongate than females. This sex difference is attributed to the need of the carapace to accommodate the large male copulatory apparatus, and the degree of dimorphism is an indication of male investment in reproduction. In this study, we examine trends in sexual dimorphism, as a proxy for sexual selection, from the Late Cretaceous to the late Eocene to better understand the long-term effects of the Cretaceous/Paleogene mass extinction. We used mixture models to identify sex clusters from digitized outlines of photographed specimens and estimated size and shape dimorphism as the difference in the mean log area and the mean log length-to-height ratio for male and female clusters. We found dimorphism exhibits a phylogenetic signal; families and genera tend to occupy various restricted subsets of dimorphism space. Previous work documented that the mean and variance in size and shape dimorphism decreased sharply at the Cretaceous/Paleogene boundary, and here we show that this fauna only partially returns to Cretaceous dimorphism patterns by the late Eocene. Most surprisingly, species with both high size and shape dimorphism, which occurred in a diverse set of taxa before the extinction, remain rare into the late Eocene. These trends suggest sexual selection may respond to several possible demographic and environmental factors, which warrant further investigation.

1. Introduction

Ostracodes are one of the few fossil taxa for which paleontologists can frequently distinguish sexes, and thereby document sexual dimorphism (Ozawa, 2013). Sex differences in ostracode carapaces were sometimes mistaken for species differences by early workers, and their recognition has led to improved species-level taxonomy (Alexander, 1932; Brouwers and Hazel, 1978; Puckett, 1996). More broadly, sexual dimorphism has been important in inferring aspects of the sexual biology of extinct ostracodes. For example, before the recent discovery of males in a living species of the Darwinulidae (Smith et al., 2006), the lack of recognized males in this clade after the Triassic had been taken as evidence for its status as a long lasting, asexual lineage (Martens et al., 2003). Inferred sex differences have also been used to document brooding of eggs or young in carapaces (Hanai, 1951; Spjeldnaes, 1951; Lethiers et al., 1997) and the presence of sexual selection in fossil populations (Yamaguchi et al., 2017).

Ostracodes of the superfamily Cytheroidea are particularly amenable to broad studies of sexual dimorphism because males in this group are generally more elongate than females (van Morkhoven, 1962; Cohen and Morin, 1990; Horne et al., 2002), a difference arising from expansion of the posterior part of the carapace that accommodates the large male copulatory organs (Horne et al., 1998; Fernandes Martins et al., 2017). Hunt et al. (2017) reported a comprehensive survey of the sexual dimorphism patterns from the Late Cretaceous of the United States Coastal Plain. They found that, given sufficient sample sizes, sexes could nearly always be distinguished from statistical analysis of valve size (measured as lateral area) and shape (measured as length-to-height ratio). The nature of this sexual dimorphism varied considerably across species within this fauna; males ranged in shape from 2% to 17%

* Corresponding author.
E-mail address: hunte@si.edu (G. Hunt).

https://doi.org/10.1016/j.marmicro.2020.101959
Received 13 August 2020; Received in revised form 22 December 2020; Accepted 29 December 2020
Available online 6 January 2021

more elongate than females, and in size from about 30% larger to 20% smaller than females. Species with larger and more elongate males had a higher probability of extinction, suggesting that high male investment in reproduction can be a detriment to species survival (Martins et al., 2018).

Subsequent work found that the distribution of sexual dimorphism contracted markedly across the Cretaceous/Paleogene boundary (K/Pg) in this fauna (Martins et al., 2020). This contraction was largely due to extinction of species in which males were much larger and much more elongate than females, demonstrating high investment in reproduction. This shift in dimorphism is consistent with the extinction selectivity observed previously during background intervals. The K/Pg interval also saw selective extinction of genera with males indicative of very low male investment (males smaller, and only slightly more elongate than

Table 1
Summary of Eocene populations analyzed for sexual dimorphism. No. of samples indicates how many samples were combined before analysis, and No. of individuals indicates the total sample size. ΔBIC measures the support for the two-group mixture model over the one-group mixture model (ΔBIC = $BIC_2 - BIC_1$). Size and shape dimorphism (DM) are measured as male minus female means.

Population Label	Species	Status	No. individuals	No. samples	ΔBIC	Size DM	Shape DM
ACA_HOWE-1	*Acanthocythereis howei* (Huff, 1970)	OK	30	1	60.0	0.0450	0.1364
ACA_SPIN-1	*Acanthocythereis spinomuralis* (Howe & Howe, 1973)	OK	30	1	8.04	0.0346	0.0662
ACT_GIBS-1	*Actinocythereis gibsonensis* (Howe & Chambers, 1935)	OK	26	1	5.82	0.0270	0.0956
ACT_GRIG-1	*Actinocythereis grigsbyi* (Howe & Chambers, 1935)	OK	30	1	13.8	0.1543	0.1402
ACT_PURI-1	*Actinocythereis purii* (Huff, 1970)	OK	35	1	65.6	0.0720	0.1589
BRA_WATE-1	*Brachycythere watervalleyensis* (Howe & Chambers, 1935)	OK	43	1	3.24	0.0952	0.0517
BUN_SHUB-1	*Buntonia shubutaensis* (Howe & Chambers, 1935)	OK	80	1	54.6	0.0153	0.1001
BUN_SMIT-1-2-3	*Buntonia smithi* (Huff, 1970)	OK	35	3	18.9	0.0870	0.0649
BUN_WARN-1	*Buntonia warneri* (Howe & Pyeatt, 1935)	OK	36	1	31.2	0.0193	0.1259
CLI_CALD-1	*Clithrocytheridea caldwellensis* (Howe & Chambers, 1935)	OK	32	1	3.19	−0.0634	0.0723
CLI_GARR-1	*Clithrocytheridea garretti* (Howe & Chambers, 1935)	OK	27	1	34.4	0.2205	0.0835
CMA_CHAM-1	*Cyamocytheridea chambersi* (Stephenson, 1937)	OK	26	1	9.30	−0.0349	0.0811
CTT_ALEX-1	*Cytheretta alexanderi* (Howe & Chambers, 1935)	OK	30	1	15.9	0.1219	0.0634
CUS_PAPU-1-2	*Cushmanidea papula* (Krutak, 1961)	OK	23	2	2.02	0.0595	0.0809
CYM_ASPE-1	*Cytheromorpha asperata* (Huff, 1970)	OK	17	1	28.3	0.1438	0.1394
CYM_CALV-1	*Cytheromorpha calva* (Krutak, 1961)	OK	14	1	25.2	0.2263	0.0737
DIG_RUSS-1	*Digmocythere russelli* (Howe & Lea, 1936)	OK	50	1	13.4	0.1577	0.0515
ECH_JACK-1	*Echinocythereis jacksonensis* (Howe & Pyeatt, 1935)	OK	38	1	39.0	0.1567	0.0782
ECH_SPA-1	*Echinocythereis spA* (Hunt & Puckett unpub)	OK	31	1	49.5	0.1629	0.0956
HAP_EHLE-1	*Haplocytheridea ehlersi* (Howe & Stephenson, 1935)	OK	40	1	41.5	0.0974	0.0679
HAP_MONT-1	*Haplocytheridea montgomeryensis* (Howe & Chambers, 1935)	OK	21	1	28.5	−0.0627	0.1385
HAZ_COUL-1-2	*Hazelina couleycreekensis* (Gooch 1939)	OK	23	2	6.98	0.0524	0.0659
HEM_BELL-1	*Hemicythere bellula* (Howe 1951)	OK	31	1	2.58	−0.0142	0.0647
HEM_CRON-1	*Hemicythere croneisi* (Huff, 1970)	OK	32	1	5.50	−0.0075	0.0793
HEN_FLOR-1-2	*Henryhowella florienensis* (Howe & Chambers, 1935)	OK	95	2	11.2	0.0072	0.1007
HEN_FLOR-3	*Henryhowella florienensis* (Howe & Chambers, 1935)	OK	36	1	32.2	0.0119	0.1017
HER_COLL-1-2	*Hermanites collei* (Gooch 1939)	OK	31	2	4.67	−0.1300	0.0661
HER_DOHM-2	*Hermanites dohmi* (Howe & Chambers, 1935)	OK	37	1	14.3	−0.0017	0.0611
HER_HYSO-1-2	*Hermanites hysonensis* (Howe & Chambers, 1935)	OK	32	2	6.63	−0.0139	0.0644
KON_SPUR-1	*Konarocythere spurgeonae* (Howe & Chambers, 1935)	OK	32	1	49.8	0.0581	0.0946
KON_SPUR-2	*Konarocythere spurgeonae* (Howe & Chambers, 1935)	OK	33	1	38.0	0.0637	0.0968
KRI_HIWA-1	*Krithe hiwanneensis* (Howe & Lea 1936)	OK	21	1	25.8	0.0174	0.1437
LOX_COCO-1	*Loxoconcha cocoaensis* (Krutak, 1961)	OK	12	1	8.63	−0.1026	0.1038
LOX_CREO-1	*Loxoconcha creolensis* (Howe & Chambers, 1935)	OK	33	1	16.4	0.1582	0.0875
LOX_JACK-1	*Loxoconcha jacksonensis* (Howe & Chambers, 1935)	OK	19	1	9.30	−0.0127	0.0719
OCC_BROU-1	*Occultocythereis broussardi* (Howe & Chambers, 1935)	OK	31	1	11.3	0.0529	0.0581
PAR_BELH-1-2	*Paracytheridea belhavenensis* (Howe & Chambers, 1935)	OK	39	2	3.56	−0.1065	0.0919
PTE_IVAN-1-2	*Pterygocythereis ivani* (Howe 1951)	OK	19	2	0.361	0.0647	0.0513
PTE_MURR-1-2-3	*Pterygocythereis murrayi* (Hill 1954)	OK	27	3	1.48	−0.0239	0.0485
TRA_BLAN-1-2	*Trachyleberidea blanpiedi* (Howe 1936)	OK	16	2	21.0	0.2292	0.0788
TRB_MONT-1	*Trachyleberis montgomeryensis* (Howe & Chambers, 1935)	OK	61	1	64.7	0.0712	0.1395
TRO_CARI-1	*Tropidocythere carinata* (Huff, 1970)	OK	17	1	3.89	−0.0704	0.0553
XES_VESC-1	*Xestoleberis vesca* (Howe & Howe, 1973)	OK	28	1	0.376	−0.0881	0.0432
ACC_COCO-1	*Acuticythereis cocoaensis* (Krutak, 1961)	some uncertainty	8	1	13.2	−0.1041	0.0859
CUS_SERA-1-2-3	*Cushmanidea serangodes* (Krutak, 1961)	some uncertainty	11	3	12.2	0.1616	0.1266
OPI_MISS-1-2	*Opimocythere mississippiensis* (Meyer, 1887)	some uncertainty	39	2	1.66	0.0707	0.0431
ABS_CARI-1-2-3	*Absonocytheropteron carinata* (Puri, 1957)	no estimates - female only	24	3	−8.85		
ABS_CARI-4	*Absonocytheropteron carinata* (Puri, 1957)	no estimates - female only	28	1	−5.57		
BUN_MORS-1	*Buntonia morsei* (Howe & Pyeatt 1935)	no estimates - female only	10	1	−1.27		
CMA_WATE-1	*Cyamocytheridea watervalleyensis* (Stephenson, 1937)	no estimates - female only	30	1	−7.25		
EUC_LOWE-1	*Eucythere lowei* (Howe, 1936)	no estimates - female only	15	1	−1.44		
CYT_LANC-1	*Cytheropteron lanceolata* (Huff, 1970)	no estimates	35	1	−3.36		
CYT_MONT-1-2-3	*Cytheropteron montgomeryensis* (Howe & Chambers, 1935)	no estimates	81	3	−8.51		
HER_DOHM-1	*Hermanites dohmi* (Howe & Chambers, 1935)	no estimates	41	1	−3.22		
TRI_GNYT-1	*Triginglymus gnythophoreus* (Krutak, 1961)	no estimates	35	1	−1.03		
CLI_GRIG-1-2	*Clithrocytheridea grigsbyi* (Howe & Chambers, 1935)	no estimates - mixed species	35	2			
LOX_CONC-1	*Loxoconcha concentrica* (Krutak, 1961)	no estimates - mixed species	44	1			

females), hinting at extinction selectivity at both ends of the male-investment continuum (Martins et al., 2020).

Here, we document sexual dimorphism patterns in cytheroid ostracodes in this same region from the late Eocene, sampling the same fauna approximately 30 Myr after the K/Pg boundary. Our goals were to assess the temporal persistence of sexual dimorphism shifts associated with the K/Pg mass extinction and to document longer term evolutionary trends in this regional fauna.

2. Methods

2.1. Fossil collections

We sampled 57 populations assigned to 53 species from the collections of Louisiana State University. All were dated to the Jacksonian regional stage of the late Eocene (~38 to 34 Ma) (Table 1). These samples were collected in Louisiana, Mississippi, and Alabama from the Moody's Branch, Danville Landing, and Yazoo Formations, the last of which was represented by its North Twistwood Creek, Cocoa Sand, Pachuta Marl, and Shubuta Members.

Data for the Late Cretaceous and early Paleocene were previously published by Hunt et al. (2017) and Martins et al. (2020), respectively. The early Paleocene dataset contains 65 populations of 47 species from the Midwayan regional stage (66 to ~59 Ma). The Late Cretaceous dataset contains 145 populations of 96 species dated from ~88 to 66 Ma.

2.2. Measuring dimorphism

We followed the same protocol for digitizing specimens and calculating dimorphism as in previous studies of these faunas (Hunt et al., 2017; Martins et al., 2020). We used a dissecting microscope to take digital photographs of each specimen in lateral view. We then used the morphometrics software TPSDig (Rohlf, 2013) to digitize the outline around each valve, including its ornamentation. *Pterygocythereis ivani,* however, has wing-like alae that obscure the carapace margin, so we digitally removed the alae from their outlines following the protocol in Hunt et al. (2017). We calculated each specimen's body size as the log area of its digitized outline. Shape was measured by fitting an ellipse to each digitized outline and then taking the log ratio of the major axis and the minor axis. The major and minor axes of the fitted ellipse are similar to the length and height measurements traditionally reported in ostracode research, but they are less subjective in that they do not require the user to specify the points at which the measurements are taken.

For each population, we used the R package *mclust* (Scrucca et al.,

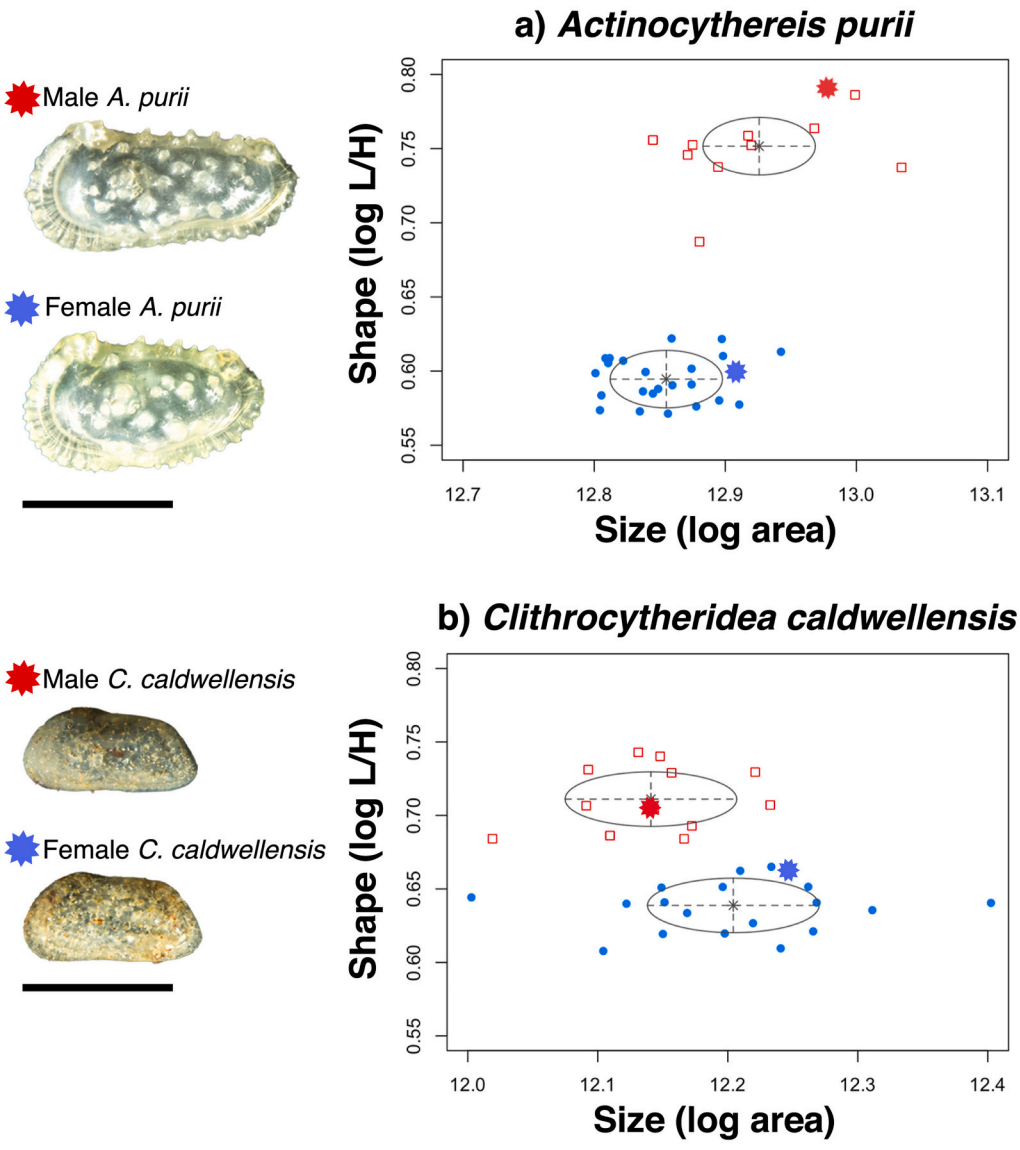

Fig. 1. Size and shape data from two populations of ostracodes from the late Eocene of the U.S. Coastal Plain. Males (red squares) and females (blue circles) shown with their 95% probability ellipses, centered on the means for each sex. Images at the left correspond to the starred individuals in the plots; scale bar is 600 μm. (a) *Actinocythereis purii*, (b) *Clithrocytheridea caldwellensis*. (For interpretation of the references to colour in this figure legend, the reader is referred to the web version of this article.)

2016) to fit mixture models to the combined size and shape data. This approach assumes that the measurements come from a mixture of bivariate normal distributions. We compared the Bayesian Information Criterion (BIC) of the one-group and two-group solutions to quantify the support for sex clusters. If BIC favored the two-group solution, we interpreted the cluster with higher L/H to be the males, because males are usually more elongate than females in living cytheroid ostracodes. We calculated each population's shape and size dimorphism as the difference between the male and female means on the shape and size axes, respectively (Fig. 1).

2.3. Statistical analyses

To better understand variation in dimorphism across taxa, we tested for linear relationships between size and shape dimorphism and mean size and shape, taken from the female cluster so as to exclude sexual dimorphism. We also tested for associations between the estimated sex ratio (proportion male) and size and shape dimorphism. These analyses were performed with populations as the units of analysis to incorporate variation within and between species. In case these relationships have varied over time, we ran separate linear models for the Eocene, Paleocene, and Cretaceous datasets, using the *lm* function from the R *stats* package (R Core Team, 2018).

All remaining analyses were conducted at the species level. Dimorphism estimates for species with multiple sampled populations were computed as the average of those populations' dimorphism estimates. In order to test for temporal changes in size and shape dimorphism, we ran multi-factor analysis of variance in which size and shape dimorphism were separately predicted by faunal age (Cretaceous, Paleocene, Eocene). In order to estimate variance explained by phylogenetic relationships, we included a term in these models for taxonomic family, lumping families represented by fewer than 8 sampled species into a category "Other." These 9 families all contained 3 or fewer sampled species, so their effects could not be estimated individually. We then repeated the linear model testing for differences among the three faunas separately for our three best-sampled families, Cytherideidae, Trachyleberididae, and Loxoconchidae. We examined pairwise differences between the temporal faunas using the function *TukeyHSD* in order to correctly account for the number of separate tests. We also plotted and qualitatively compared dimorphism in families with at least 8 species and genera with at least 5 species.

We used the *var.test* function from the R *stats* package to do an *F*-test for differences in dimorphism variance among the three time intervals. F-tests can only test for differences between pairs of populations, so we ran the test for each pairwise combination of the Cretaceous, Paleocene, and Eocene datasets.

For all linear models, we assessed whether the model residuals were distributed normally, as is assumed by this approach. In cases in which residuals were significantly non-normal according to a Shapiro-Wilk test, we report *P*-values from a permutation test rather than the parametric result, using the *perm.anova* function from the R package *RVAideMemoire* (Hervé, 2020). For all tests, we used a two-tailed alpha value of 0.05.

Finally, we examined the frequency of high-male-investment dimorphism, in which males are much larger and much more elongate than females. We followed Martins et al. (2020) in considering species with both size dimorphism and shape dimorphism higher than the Cretaceous medians to have high male investment. We counted the proportion of such species in each of the Eocene, Paleocene, and Cretaceous datasets. We used the Cretaceous medians as our point of reference to see if the sudden reduction in high male investment after the K/Pg extinction persisted into the late Eocene.

3. Results

3.1. Dimorphism estimates

We were able to estimate shape and size dimorphism for 46 Eocene populations assigned to 44 species (Table 1, Figs. 1-2). Eleven other populations did not result in clear two-group sex clusters. Five of these populations favored a one-group solution and exhibited the limited variance in shape typical of a single sex, which indicates they are likely all-female, parthenogenic populations (Hunt et al., 2017, p. 16–17). Some of the remaining six populations had modest sample size or evidence of mixed species composition that likely explain the failure to find sex clusters. Only the 46 populations for which we obtained dimorphism estimates were used in subsequent analyses.

3.2. Correlates of dimorphism

Size and shape dimorphism were not consistently correlated with average female size, average female shape, sex ratio, or each other over time (Table 2). Size dimorphism and shape dimorphism are significantly correlated in the Cretaceous and the Paleocene, but the relationships are weak and in opposite directions. Only in the Paleocene was size dimorphism significantly correlated with valve shape and valve size, and only in the Cretaceous was shape dimorphism significantly correlated with valve shape and sex ratio. In both the Cretaceous and the Paleocene, shape dimorphism and valve size are negatively correlated. Even these statistically significant correlations, however, explain less than 13% of variability in the data. Population sex ratios are generally female-biased, with a spread that converges with increasing sample size to a proportion male of about 0.4 (Fig. 3).

3.3. Variation in dimorphism across time periods

After a significant drop from the Cretaceous to the Paleocene (Martins et al., 2020), shape dimorphism increased slightly by the late Eocene (Table 3) to a value intermediate between the two earlier periods and significantly different from neither (Eocene-Cretaceous $P = 0.149$, Eocene-Paleocene: $P = 0.841$). Size dimorphism also decreased, albeit non-significantly, from the Cretaceous to the Paleocene, with an additional but smaller decrease from the Paleocene to the late Eocene (Table 3). Mean size dimorphism is not significantly different in the Eocene compared to the previous periods (Eocene-Cretaceous $P = 0.200$, Eocene-Paleocene: $P = 0.935$).

In addition to changes in mean dimorphism across the K/Pg boundary, dispersion also decreased (Fig. 4, Table 3). Variance in both size dimorphism ($F_{46,95} = 0.521$, $P = 0.016$) and shape dimorphism ($F_{46,95} = 0.517$, $P = 0.015$) decreased between the Cretaceous and Paleocene. By the late Eocene, however, variance in shape dimorphism was greater than that in the Paleocene ($F_{43,46} = 2.18$, $P = 0.0102$), rebounding to a level similar to the Cretaceous (Table 3). Eocene variance in size dimorphism shifted to a level intermediate between that of the Cretaceous and the Paleocene and not statistically significantly different from either (Cretaceous-Eocene: $F_{43,95} = 0.684$, $P = 0.167$; Paleocene-Eocene: $F_{43,46} = 1.31$, $P = 0.365$).

Size and shape dimorphism exhibit a phylogenetic signal, differing by family (Size: $F_{13,161} = 3.36$, $P = 0.00014$; Shape: $F_{13,161} = 3.51$, $P =$ 7.8e-5). In general, families' long-term dimorphism trends depend on their initial dimorphism (Fig. 5). For Cytherideidae, a permutation test showed that mean shape dimorphism changed over time ($F_{2,36} = 13.3$, $P = 0.002$). The variance in shape dimorphism within this family also decreased between the Cretaceous and Paleocene ($F_{13,19} = 0.136$, $P =$ 6.9e-4) and then increased between the Paleocene and Eocene ($F_{4,13} =$ 11.3, $P =$ 7.0e-4). For Trachyleberididae and Loxoconchidae, mean dimorphism did not differ statistically significantly among these time periods. However, variance in size dimorphism for the Loxoconchidae increased between the Cretaceous and Eocene ($F_{4,4} = 27.1$, $P = 0.0074$).

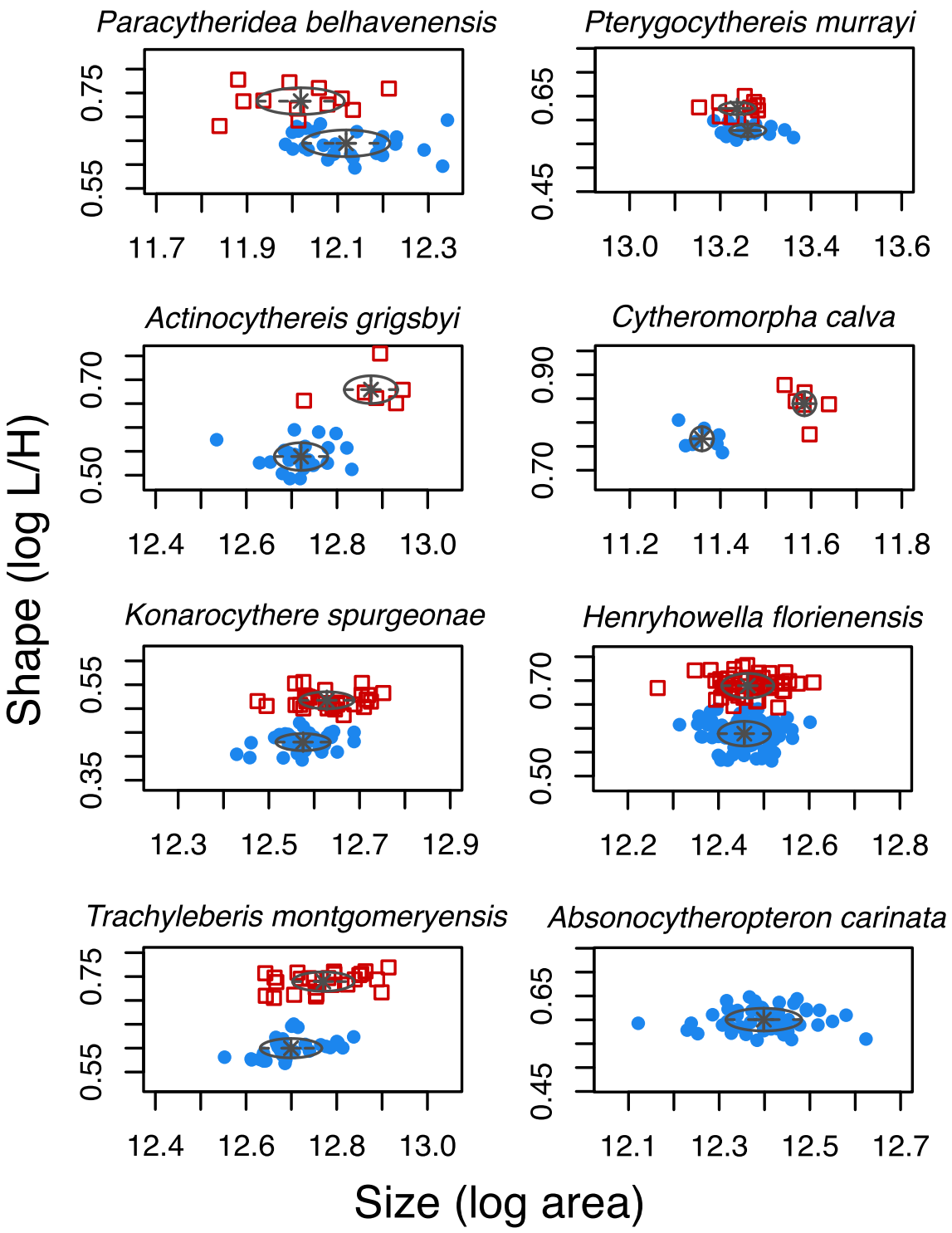

Fig. 2. Male (red squares) and female (blue circles) sex clusters for eight additional populations from the Eocene. Axis limits were set so that each panel spans the same range of shape and size dimorphism, which makes within-panel distances comparable across panels. *Absonocytheropteron carinata* is an example of a population interpreted to be entirely female. (For interpretation of the references to colour in this figure legend, the reader is referred to the web version of this article.)

For Trachyleberididae, variance in shape dimorphism also increased between the Paleocene and Eocene ($F_{21,19} = 2.49$, $P = 0.0499$).

3.4. Frequency of high male investment dimorphism

As previously reported (Martins et al., 2020), the frequency of species with high male-investment dimorphism (i.e., those with dimorphism greater than the Cretaceous medians for size and shape) is high in the Cretaceous and extremely low in the early Paleocene (Fig. 4). In the Late Cretaceous, a third of all species fall into this upper-right quadrant of Fig. 4, whereas only one species (2.1%) in the Paleocene does. This frequency increases somewhat in the late Eocene with 3 species (6.8%) in this region, but this proportion is still far lower than that observed in the Cretaceous. The three species with high male investment in the late Eocene – *Cytheromorpha asperata*, *Actinocythereis grigsbyi*, and *Cushmanidea serangodes* – are all from different families, and therefore

Table 2
Results of linear models for morphological correlates of sexual dimorphism for the Late Cretaceous ($n = 145$), early Paleocene ($n = 65$), and late Eocene ($n = 46$). Significant results ($P < 0.05$) are in bold.

	Eocene		Paleocene		Cretaceous	
	r	P-value	r	P-value	r	P-value
Shape DM v. Size DM	0.105	0.486	**−0.295**	**0.0172**	**0.334**	**4.10E-05**
Size DM v. Valve Size	0.167	0.273	**0.289**	**0.0196**	−0.0134	0.873
Size DM v. Valve Shape	0.0519	0.735	**−0.330**	**0.00730**	−0.0945	0.258
Size DM v. Sex Ratio	−0.151	0.316	−0.0916	0.468	−0.00422	0.960
Shape DM v. Valve Size	−0.0465	0.762	**−0.333**	**0.00664**	**−0.350**	**1.60E-05**
Shape DM v. Valve Shape	−0.0654	0.670	0.130	0.303	**−0.234**	**0.00455**
Shape DM v. Sex Ratio	−0.225	0.133	−0.0492	0.697	**−0.215**	**0.00923**

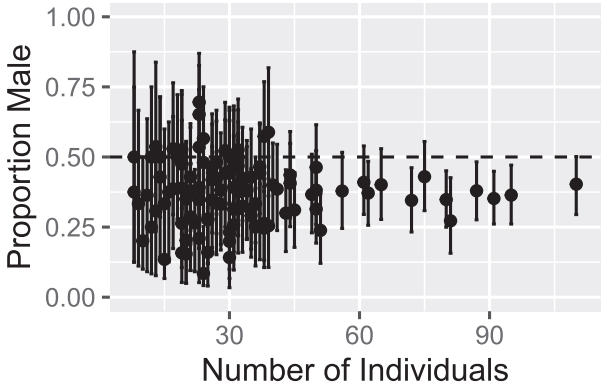

Fig. 3. As sample size increases, populations' sex ratios (proportion specimens that are male) converge to about 0.4 (Eocene and Paleocene data). Error bars represent 95% confidence intervals generated through parametric bootstrapping of the mixture model fitting.

Table 3
Means and standard deviations of size and shape dimorphism in species from the Late Cretaceous ($n = 96$), early Paleocene ($n = 47$), and late Eocene ($n = 44$). The change in mean shape dimorphism between the Cretaceous and Paleocene is statistically significant, as are the changes in variance for shape and size dimorphism between the Cretaceous and Paleocene, and variance in shape dimorphism between the Paleocene and Eocene (summary statistics reported in the text).

	Size dimorphism		Shape dimorphism	
	mean	std. dev.	mean	std. dev.
Eocene	0.046	0.094	0.086	0.031
Paleocene	0.053	0.082	0.083	0.021
Cretaceous	0.076	0.114	0.096	0.029

independently evolved this style of sexual dimorphism.

3.5. Dimorphism in specific taxa

Two families, Trachyleberididae and Cytherideidae, account for 75% of species in our dataset, with 101 and 39 species, respectively. Both have species with a variety of dimorphism patterns, including those with low and high sexual dimorphism (Fig. 5). The Cytherideidae has a narrower range, however, as this family lacks species with shape dimorphism much lower than 0.07. The Trachyleberididae shows a marked contraction in the upper-right and lower-left of the dimorphism space from the Cretaceous to the Paleocene, with only a partial recovery of these areas by the late Eocene (Fig. 5). Loxoconchid species are characterized by moderate to strong sexual dimorphism, whereas all sampled Hemicytheridae have modest shape dimorphism and size dimorphism close to zero (Fig. 5). Males in the Cytheruridae are usually smaller than females, although often markedly more elongate in shape.

Among the nine genera for which we sampled at least five species, *Haplocytheridea*, *Hazelina*, and *Cytheromorpha* all show quite strong size and shape dimorphism (Fig. 6), with *Haplocytheridea* and *Hazelina* showing marked decreases in dimorphism after the Cretaceous. *Brachycythere* shows high size dimorphism but average shape dimorphism. *Loxoconcha*, *Acanthocythereis*, *Clithrocytheridea*, *Hermanites*, and *Pterygocythereis* show average size and shape dimorphism, though they differ in their spread. These less dimorphic genera show smaller changes over time.

4. Discussion

4.1. Temporal changes in sexual dimorphism

The K/Pg corresponds with a marked decrease in shape dimorphism, a similar but statistically nonsignificant decrease in size dimorphism, and a decrease in dimorphism variance (Martins et al., 2020). In the late Eocene, ~30 million years after the K/Pg, we find that cytheroid ostracodes show a partial return to Cretaceous-like patterns of sexual dimorphism. Eocene shape and size dimorphism are not notably different from that observed in the Cretaceous or Paleocene. Variance in shape dimorphism increased between the Paleocene and Eocene, back to Cretaceous levels, whereas variance in size dimorphism only partially rebounded.

The extreme combination of both high shape and high size dimorphism, which was relatively common in the Cretaceous, remains rare in the Eocene. While a third of Cretaceous species were above both the median shape and size dimorphism, only one Paleocene and three Eocene species fall above both Cretaceous medians. Thus, between the end of the Cretaceous and the end of the Eocene, there have been few evolutionary transitions that resulted in dimorphism indicative of high male investment. In contrast, such transitions were relatively frequent in the Late Cretaceous, judging by the occurrence of this style of dimorphism in 32 species from 14 different genera (Martins et al., 2020). The persistent rarity of species with high male investment until the end of the Eocene is a puzzle for which we do not have a clear explanation. However, it may be useful to consider what factors influence sexual dimorphism more broadly in animals, and how that body of work relates to what is known about the biology of sexual dimorphism in ostracodes.

4.2. Determinants of sexual dimorphism

The relatively more elongate carapace of male cytheroid ostracodes has long been attributed to the need to accommodate the large hemipenis of males, the bulk of which consists of a large, muscular sperm pump (van Morkhoven, 1962; Cohen and Morin, 1990; Horne et al., 1998). The degree of carapace sexual dimorphism might therefore be expected to reflect variation in the size of this sperm pump. Consistent with this claim is the finding that male carapace size within several

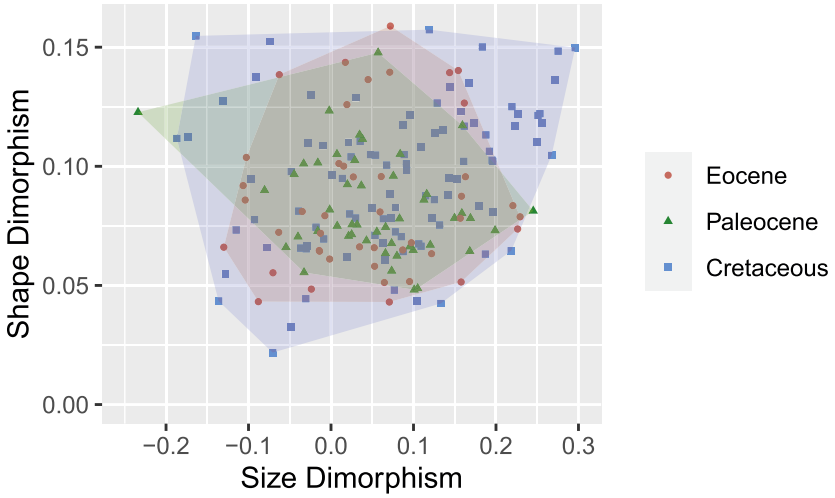

Fig. 4. Shape dimorphism with respect to size dimorphism for species from all three time periods. Dimorphism values represent male minus female means for size (log[Area]) and shape (log[L/H]).

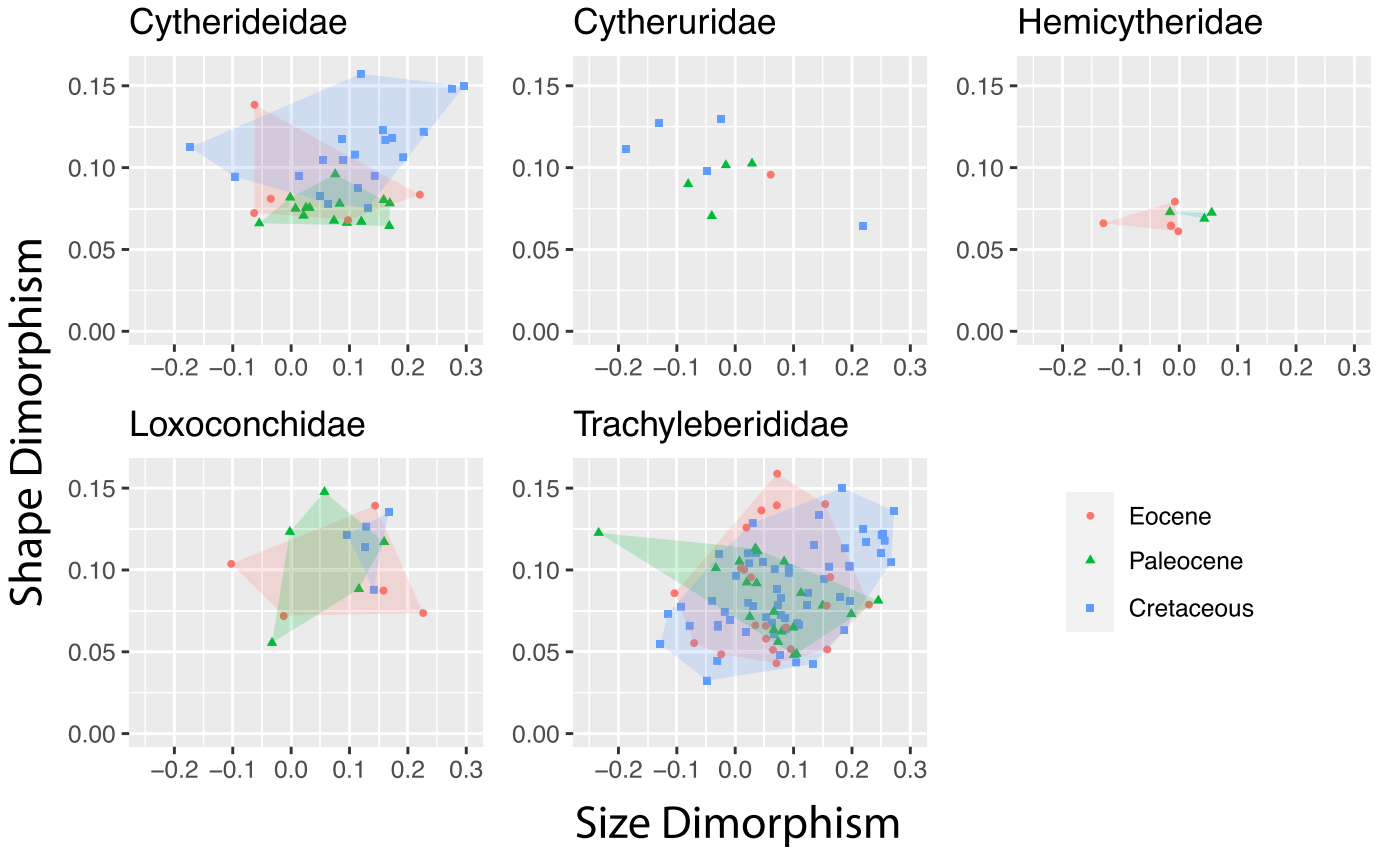

Fig. 5. Shape dimorphism versus size dimorphism for the 5 families represented by at least 8 species with dimorphism estimates. Dimorphism values represent male minus female means for size (log[Area]) and shape (log[L/H]). Convex hulls omitted from Cytheruridae plot to keep the single Eocene species visible.

species of *Cyprideis* is related to the size of this sperm pump, even after accounting for overall size of softparts (Martins et al., 2017). Other studies have related male carapace shape to the relative size of male copulatory structures (Danielopol, 1980; Kamiya, 1992).

Carapace dimorphism is likely related to male reproductive investment, but it remains unclear under what conditions male investment is expressed as increased shape dimorphism versus size dimorphism, or both. Many genera seem to vary freely in both kinds of dimorphism, whereas others, such as *Clithrocytheridea* and *Hermanites*, vary substantially in size dimorphism but hardly differ in shape dimorphism (Fig. 6). We know of no genera that appear to have the opposite pattern of highly variable shape dimorphism but little variation in size dimorphism. The explanation for these patterns is not clear, but the evolutionary response in the carapace to selection on male investment may depend on sexual or other forms of natural selection acting on aspects of the carapace. For example, stabilizing natural selection on male body shape, coupled with sexual selection favoring increased male reproductive investment, may result in an evolutionary response

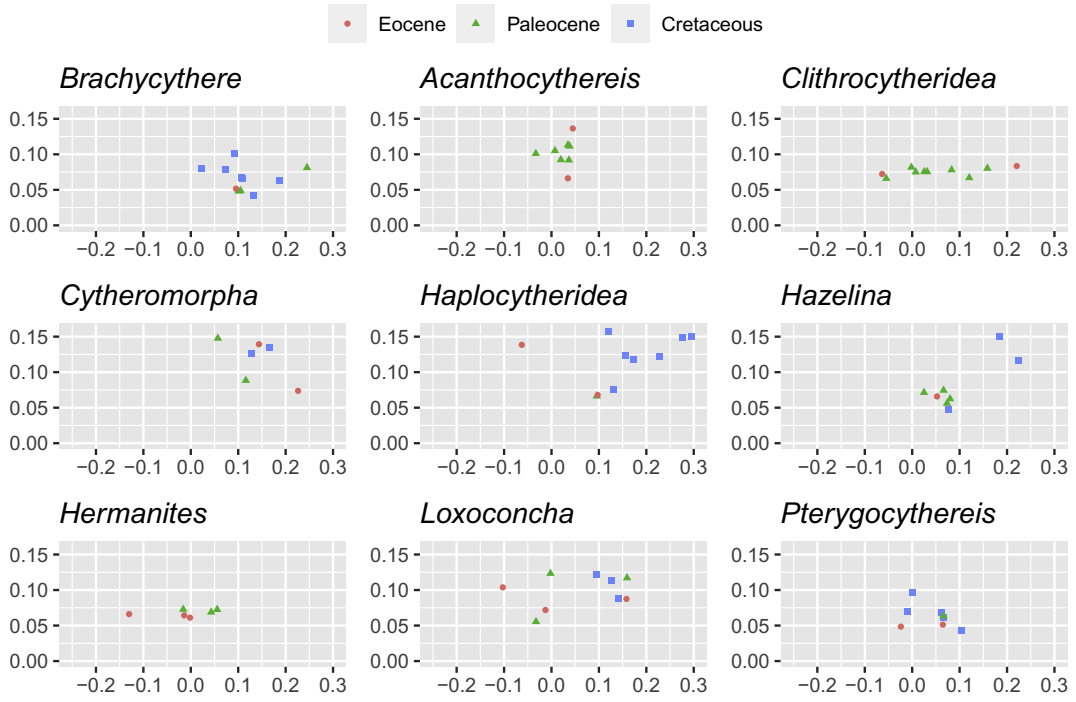

Fig. 6. Shape dimorphism versus size dimorphism for the 9 genera with over 5 species with dimorphism estimates. Dimorphism values represent male minus female means for size (log[Area]) and shape (log[L/H]).

predominantly in carapace size. Further comparative studies of carapace dimorphism in extant ostracode taxa, and its relationship to soft anatomy, might help resolve this question.

The connection between carapace dimorphism and sperm pump features suggests that the degree of dimorphism is related to the volume of the ejaculate, the number or size of sperm cells in the ejaculate, and/or the generation of forces by the sperm pump to aid the transfer of sperm to the female's seminal receptacle. These factors are all important in sperm competition, a form of sexual selection that occurs when sperm from more than one male compete to fertilize eggs of a female (Parker, 1970). Sperm competition can arise whenever females mate with multiple males, which has been observed in living ostracodes (Abe and Vannier, 1991). Moreover, in many animal taxa, male reproductive investment is consistently higher in species whose mating systems and reproductive behavior result in frequent multiple matings per female (Simmons and Fitzpatrick, 2012; Parker, 2016; Baker and Shackelford, 2018; Rowley et al., 2019). Sperm structure is highly variable across cytheroids (Wingstrand, 1988). To the extent that these structural features influence sperm's ability to successfully reach and fertilize an egg, their divergence across taxa may be the result of frequent sperm competition operating within cytheroid lineages.

Male reproductive investment often manifests as the production of more sperm, as would be reflected in measures such as relative testes mass. However, sperm competition in small-bodied animals can sometimes result in sperm that are individually large, rather than more numerous (Immler et al., 2011; Godwin et al., 2017). This trend is taken to the extreme in a different clade of ostracodes, the Cypridoidea, in which sperm are commonly longer than 1 mm in length – often longer than the total length of the animal – with a maximum reported length of nearly 12 mm (Matzke-Karasz, 2005; Smith et al., 2014). While cytheroids lack these truly giant sperm, their sperm can still be quite large. Wingstrand's (1988) compilation of sperm data from 22 cytheroid species reported an average sperm length of 112 μm, with a maximum of 440 μm, which represent substantial fractions of total body length (mostly between 400 and 1000 μm in this superfamily). Comparative data on sperm size, along with carapace size and shape in males and females, would help to determine if carapace dimorphism is related to sperm size or sperm quantity. Such data are available for cypridoids (Smith et al., 2014), but to our knowledge no comparable datasets exist for cytheroids.

Our discussion of the causes of carapace dimorphism thus far has followed the traditional view among ostracode workers that sex differences are caused largely by male reproductive function. Much less considered is the potential for other functions to shape carapace dimorphism. Carapace shape has been suggested to influence the mechanics of copulation (Kamiya, 1988), possibly leading to different optimal shapes in males and females. It is also conceivable that reproductive investment by females could lead to adaptive modifications to carapace shape. Such investment could take the form of increased numbers or sizes of eggs, for example, or in the brooding of young inside the carapace. Brooding is thought to result in carapaces that are wider laterally in females, rather than affecting the lateral views we capture here (Ozawa, 2013), but this suggestion has not been thoroughly tested. Brooding occurs in cytheroids, but it is uncommon (Cohen and Morin, 1990). Among the genera included here, only *Xestoleberis* is known to brood young in the female carapace among its living species. Several extant genera within the Cytherideidae brood, and so it is possible that some of the extinct cytherideid genera encountered here, such as *Vetustocytheridea*, also brooded. Finally, carapace shape very likely modulates other, non-sexual functions as well. Previous work has suggested adaptive differences in shape between species living in different habitats (Kamiya, 1988; Tanaka, 2009). Unless males and females have differing habitat preferences, however, these adaptive differences are unlikely to affect differences between the sexes.

While acknowledging the above uncertainties, we suggest that the link between carapace dimorphism and male reproductive investment is likely to be broadly valid in cytheroids. Given the consistent relationship between male investment and the frequency of multiple matings among females noted above, a next step is to consider what factors influence the rate at which females mate with multiple males. Studies on other animal taxa have explored a variety of such determinants, including mating system (Adams et al., 2020), local group size and number of females in

mating aggregations (Isvaran and Clutton-Brock, 2007; Adams et al., 2020), length of the breeding season (Isvaran and Clutton-Brock, 2007), and adult mortality rate (Griffith et al., 2002), none of which can be readily studied in extinct taxa. Although some studies characterize aspects of the reproductive biology of specific living cytheroid species (e.g., Horne, 1983; Kamiya, 1988; Cohen and Morin, 1990), there are few such studies, probably because studying behavior in tiny, marine organisms is inherently challenging. Other potential factors influencing male reproductive investment are potentially more amenable to paleontological analysis. It has been suggested that the opportunity for multiple mating is higher at high population density (Friesen and Shine, 2019), although this relationship does not appear to be very general, at least in birds (Griffith et al., 2002). Operational sex ratio can be investigated in ostracodes (Abe, 1983, 1990), and it may influence mating frequencies, and thus the potential for sperm selection. We find little indication of a consistent relationship between sex ratio and sexual dimorphism here (Table 2), although power is limited by the broad confidence intervals around estimates of sex ratio (Fig. 2). Moreover, sex ratios in time-averaged fossil samples can differ from those in living populations, because the former represents the sex ratio in newly molted adults, and thus can miss the sex-biasing effects of preferential male mortality in adults (Abe, 1990). There are also examples of male investment changing consistently along environmental gradients, at least among vertebrates (Snell-Rood and Badyaev, 2008; Jin et al., 2016) and insects (Miller and Svensson, 2014), but it is not clear how common such patterns are. Future studies can explore if sexual dimorphism is correlated with relative abundance or if any of the variation in dimorphism can be explained by ecological tradeoffs between sexual selection and environmental variables such as predation or food availability.

In some animal taxa, the magnitude of sexual size dimorphism is greater in species that are of larger body size when males are the larger sex, a regularity that is known as Rensch's rule (Abouheif and Fairbairn, 1997). We find little evidence here that either overall body size or shape is important in structuring or constraining sexual dimorphism in cytheroid carapaces. Thus, the evolutionary changes in sexual dimorphism that we can document in the fossil record are more likely to be shaped by factors related to multiple matings, discussed above, that are important in shaping the intensity of sperm selection in these ostracodes. At present, we do not know which of these may be the most important, but progress may be made by targeted study of those factors that leave a trace in the fossil record or by additional studies of the mating and reproductive behavior of living cytheroids. Such inquiries might help explain the persistent shift after the K/Pg extinction away from dimorphism indicative of high male reproductive investment, and thus away from regimes characterized by the most intense sperm competition. Regardless of which traits or environmental shifts triggered this change, however, this long-term change in sexual selection represents a potentially important evolutionary shift in the history of cytheroid ostracodes.

Data availability

Eocene dimorphism data needed to reproduce these analyses are presented in Table 1. Data for the Late Cretaceous and early Paleocene are available from Hunt et al. (2017) and Martins et al. (2020), respectively.

Declaration of Competing Interest

The authors declare that they have no known competing financial interests or personal relationships that could have appeared to influence the work reported in this paper.

Acknowledgments

This research was supported by a grant from the National Science Foundation (NSF-EAR 1424906), as well as by funding from the National Museum of Natural History and Smithsonian Institution. MSF worked on this project as a participant in the Natural History Research Experience REU program (NSF-OCE 1560088) at the National Museum of Natural History. We thank C. Sanford (NMNH) and L. Smith (LSU) for assistance with collections, and T. M. Puckett for helpful discussion about this project. We thank G. Tanaka and an anonymous reviewer for their careful reading and comments on the manuscript.

References

Abe, K., 1983. Population structure of *Keijella bisanensis* (Okubo) (Ostracoda, Crustacea) – an inquiry into how far the population structure will be preserved in the fossil record. J. Faculty Sci. Univ. Tokyo Section II Geol. Mineral. Geogr. Geophys. 20, 443–488.
Abe, K., 1990. What the sex ratio tells us: A case from marine ostracods. In: Whatley, R., Maybury, C. (Eds.), Ostracoda and Global Events. Chapman and Hall, London, pp. 175–185.
Abe, K., Vannier, J., 1991. Mating behavior in the podocopid ostracode *Bicornucythere bisanensis* (Okubo, 1975): rotation of a female by a male with asymmetric 5th limbs. J. Crustac. Biol. 11, 250–260.
Abouheif, E., Fairbairn, D.J., 1997. A comparative analysis of allometry for sexual size dimorphism: Assessing Rensch's rule. Am. Nat. 149, 540–562.
Adams, D.M., Nicolay, C., Wilkinson, G.S., 2020. Patterns of sexual dimorphism and mating systems. In: Fleming, T.H., Davalos, L.M., Mello, M. (Eds.), Phyllostomid Bats, a Unique Mammalian Radiation. University of Chicago Press, Chicago.
Alexander, C.I., 1932. Sexual dimorphism in fossil Ostracoda. Am. Midl. Nat. 12, 302–310.
Baker, R.R., Shackelford, T.K., 2018. Paternity data and relative testes size as meaures of level of sperm competition in the Cercopithecoidea. Am. J. Primatol. 80.
Brouwers, E.M., Hazel, J.E., 1978. Ostracoda and correlation of the Severn Formation (Navarroan; Maestrichtian) of Maryland. J. Paleontol. Suppl. 52, 1–52.
Cohen, A.C., Morin, J.G., 1990. Patterns of reproduction in ostracodes: a review. J. Crustac. Biol. 10, 184–211.
Danielopol, D.L., 1980. On the carapace shape of some European freshwater interstitial Candoninae (Ostracoda). Proc. Biol. Soc. Wash. 93, 743–756.
Fernandes Martins, M.J., Hunt, G., Lockwood, R., Swaddle, J.P., Horne, D.J., 2017. Correlation between investment in sexual traits and valve sexual dimorphism in Cyprideis species (Ostracoda). PLoS One 12, e0177791.
Friesen, C.R., Shine, R., 2019. At the invasion front, male cane toads (*Rhinella marina*) have smaller testes. Biol. Lett. 15, 1–5.
Godwin, J.L., Vasudeva, R., MIchalczyk, L., Martin, O.Y., Lumley, A.J., CHapman, T., Gage, M.J.G., 2017. Experimental evolution reveals that sperm competition intensity selects for longer, more costly sperm. Evol. Lett. 1-2, 102–113.
Griffith, S.C., Owens, I.P.F., Thuman, K.A., 2002. Extra pair paternity in birds: a review of interspecific variation and adaptive function. Mol. Ecol. 11, 2195–2212.
Hanai, T., 1951. Cretaceous non-marine Ostracoda from the Sungai Group in Manchuria. J. Faculty Sci. Univ. Tokyo Sect. II 7, 403–430.
Hervé, M., 2020. RVAideMemoire: Testing and Plotting Procedures for Biostatistics (0.9-77 ed).
Horne, D.J., 1983. Life-cycles of podocopid Ostracoda–a review (with particular reference to marine and bracksih water species). In: Maddocks, R.F. (Ed.), Applications of Ostracoda. University of Houstin Geoscience, Houstin, pp. 581–590.
Horne, D.J., Danielopol, D.L., Martens, K., 1998. Reproductive behavior. In: Martens, K. (Ed.), Sex and Parthenogenesis. Evolutionary Ecology of Reproductive Modes in Non-marine Ostracods. Backhuys Publishers, Leiden, pp. 157–195.
Horne, D.J., Cohen, A., Martens, K., 2002. Taxonomy, morphology and biology of Quaternary and living Ostracoda. In: Holmes, J.A., Chivas, A.R. (Eds.), The Ostracoda. Applications in Quaternary Research. American Geophysical Union, Washington, DC.
Howe, H.V., 1936. Ostracoda of the genus *Eucythere* from the Tertiary of Mississippi. J. Paleontol. 10, 143–145.
Howe, H.V., Chambers, J., 1935. Louisiana Jackson Eocene Ostracoda. Louisiana Department of Conservation Geological Bulletin 5, 1–65.
Howe, R.C., Howe, H.J., 1973. Ostracodes from the Shubuta Clay (Tertiary) of Mississippi. J. Paleontol. 47, 629–657.
Huff, W.J., 1970. The Jackson Eocene Ostracoda of Mississippi. Bulletin of the Mississippi Geological, Economic and Topographical Survey 114, 1–289.
Hunt, G., Martins, M.J.F., Puckett, T.M., Lockwood, R., Swaddle, J.P., Hall, C.M.S., Stedman, J., 2017. Sexual dimorphism and sexual selection in cytheroidean ostracodes from the Late Cretaceous of the U.S. Coastal Plain. Paleobiology 43, 620–641.
Immler, S., Pitnick, S., Parker, G.A., Durrant, K.L., Lupold, S., Calhim, S., Birkhead, T.R., 2011. Resolving variation in the reproductive tradeoff between sperm size and number. Proc. Nat. Acad. Sci. USA 108, 5325–5330.
Isvaran, K., Clutton-Brock, T., 2007. Ecological correlates of extra-group paternity in mammals. Proc. Royal Soc. B-Biol. Sci. 274, 219–224.
Jin, L., Yang, S.N., Liao, W.B., Lüpold, S., 2016. Altitude underlies variation in the mating system, somatic condition, and investment in reproductive traits in male Asian grass frogs (*Fejervarya limnocharis*). Behav. Ecol. Sociobiol. 70, 1197–1208.
Kamiya, T., 1988. Morphological and ethological adaptations of Ostracoda to microhabitats in *Zostera* beds. In: Hanai, T., Ikeya, N., Ishizaki, K. (Eds.), Evolutionary Biology of Ostracoda. Elsevier, Kodansha, Japan, pp. 303–318.

Kamiya, T., 1992. Heterochronic dimorphism of *Loxoconcha uranouchiensis* (Ostracoda) and its implications for speciation. Paleobiology 18, 221–236.
Krutak, P.R., 1961. Jackson Eocene Ostracoda from the Cocoa Sand of Alabama. J. Paleontol. 35, 769–788.
Lethiers, F., Damotte, R., Whatley, R., 1997. Evidence of brooding in Permian non-marine Ostracoda. Lethaia 29, 219–223.
Martens, K., Rosetti, G., Horne, D.J., 2003. How ancient are ancient asexuals? Proc. Royal Soc. B-Biol. Sci. 270, 723–729.
Martins, M.J.F., Hunt, G., Lockwood, R., Swaddle, J.P., Horne, D.J., 2017. Correlation between investment in sexual traits and valve sexual dimorphism in *Cyprideis* species (Ostracoda). PLoS One 12, e0177791.
Martins, M.J.F., Puckett, T.M., Lockwood, R., Swaddle, J.P., Hunt, G., 2018. High male sexual investment as a driver of extinction in fossil ostracods. Nature 556, 366–369.
Martins, M.J.F., Hunt, G., Thompson, C.M., Lockwood, R., Swaddle, J.P., Puckett, T.M., 2020. Shifts in sexual dimorphism across a mass extinction in ostracods: implications for sexual selection as a factor in extinction risk. Proc. Royal Soc. B-Biol. Sci. 287 (28720200730).
Matzke-Karasz, R., 2005. Giant spermatozoon coiled in small egg: Fertilization mechanisms and their implications for evolutionary studies on ostracoda (crustacea). J. Exp. Zool. B Mol. Dev. Evol. 304B, 129–149.
Meyer, O., 1887. Beitrag zur Kenntnis der Fauna der Alteriars von Mississippi und Alabama. Bericht über die Senckenbergische naturforschende Gesellschaft 1–20.
Miller, C.W., Svensson, E.I., 2014. Sexual selection in complex environments. Annu. Rev. Entomol. 59, 427–445.
Ozawa, H., 2013. The history of sexual dimorphism in Ostracoda (Arthropoda, Crustacea) since the Palaeozoic. In: Moriyama, H. (Ed.), Sexual Dimorphism. InTech, pp. 51–80.
Parker, G.A., 1970. Sperm competition and its evolutionary consequences in the insects. Biol. Rev. 45, 525–567.
Parker, G.A., 2016. The evolution of expenditure on testes. J. Zool. 298, 3–19.
Puckett, T.M., 1996. Ecological atlas of Upper Cretaceous ostracodes of Alabama. Geol. Surv. Alabama Monogr. 14, 1–176.
Puri, H.S., 1957. Stratigraphy and zonation of the Ocala Group. Florida Geological Survey Bulletin 38, 5–248.
R Core Team, 2018. R: A Language and Environment for Statistical Computing. R Foundation for Statistical Computing, Vienna, Austria.
Rohlf, F.J., 2013. tpsDIG, 2.17 ed. SUNY Stonybrook.
Rowley, A.G., Daly-Engel, T.S., Fitzpatrick, J.L., 2019. Testes size increases with sperm competition risk and intensity in bony fish and sharks. Behav. Ecol. 30, 364–371.
Scrucca, L., Fop, M., Murphy, B., Raftery, A., 2016. mclust 5: clustering, classification and density estimation using gaussian finite mixture models. R J. 8, 289–317.
Simmons, L.W., Fitzpatrick, J.L., 2012. Sperm wars and the evolution of male fertility. Reproduction 144, 519–534.
Smith, R.J., Kamiya, T., Horne, D.J., 2006. Living males of the 'ancient asexual' Darwinulidae (Ostracoda : Crustacea). Proc. Royal Soc. B-Biol. Sci. 273, 1569–1578.
Smith, R.J., Matzke-Karasz, R., Kamiya, T., de Deckker, P., 2014. Sperm lengths of non-marine cypridoidean ostracods (Crustacea). Acta Zool. 97, 1–17.
Snell-Rood, E.C., Badyaev, A.V., 2008. Ecological gradient of sexual selection: elevation and song elaboration in finches. Oecologia 157, 545–551.
Spjeldnaes, N., 1951. Ontogeny of *Beyrichia jonesi*. J. Paleontol. 25, 745–755.
Stephenson, M.B., 1937. Middle Tertiary Ostracoda of the genus *Cytheridea*. J. Paleontol. 11, 145–159.
Tanaka, G., 2009. Adaptive modifications of carapace outlines in the Cytheroidea. Biol. J. Linn. Soc. 97, 810–821.
van Morkhoven, F.P.C.M., 1962. Post-Paleozoic Ostracoda. Elsevier Publishing Company, Amsterdam.
Wingstrand, K.G., 1988. Comparative spermatology of the Crustacea Entomostraca: 2. Subclass Ostracoda. Biologiske Skrifter 32, 1–149.
Yamaguchi, T., Honda, R., Matsui, H., Nishi, H., 2017. Sexual shape dimorphism and selection pressure on males in fossil ostracodes. Paleobiology 43, 407–424.